PROCEEDINGS
30th RCI International Convention and Trade Show

Development of a Standard Test Method to Determine the Wind Resistance of Vegetated Roof Assemblies

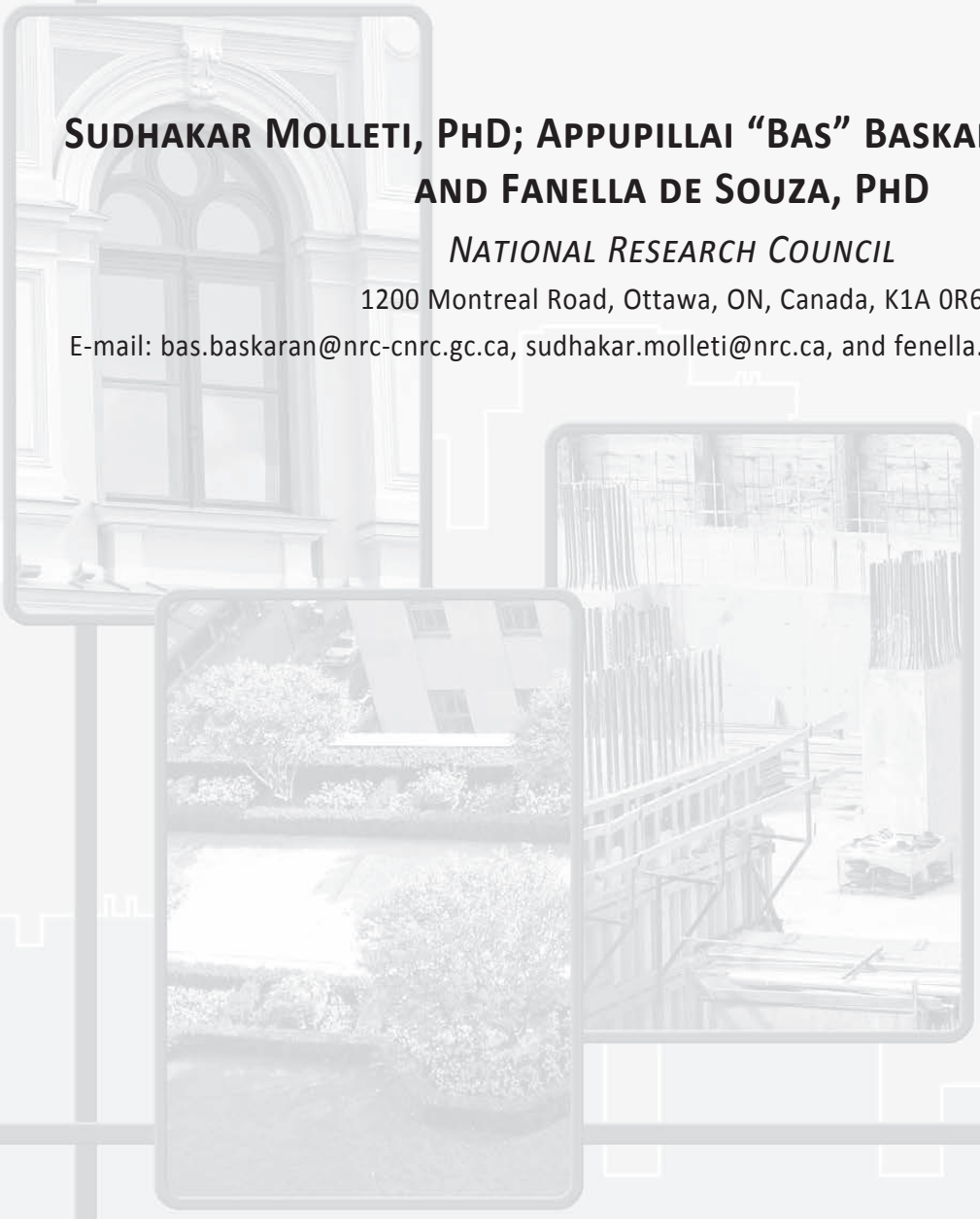

Sudhakar Molleti, PhD; Appupillai "Bas" Baskaran, PhD, PEng; and Fanella de Souza, PhD

National Research Council

1200 Montreal Road, Ottawa, ON, Canada, K1A 0R6

E-mail: bas.baskaran@nrc-cnrc.gc.ca, sudhakar.molleti@nrc.ca, and fenella.desouza@nrc-cnrc.gc.ca

Abstract

Every building has a roof system (RS). Vegetated systems (VS) consist of a variety of components such as growing media, a drainage layer, and plants. These components are intentionally placed on the rooftop to form a vegetated roof assembly (VRA), mostly on low-sloped commercial roofs. Statistics indicate that in North America, VRA market share expands with the help of federal legislation, local government incentives, and advanced research. The city of Toronto became the first major municipality in North America to mandate that new developments should cover 60% of their roof area with vegetated systems. These laws are indeed a breakthrough for an inexpensive adaptation strategy of VRA for urban areas. However, technical information on the coherent performance of vegetated systems and their impact on roofing systems' durability—especially for wind forces—is not available. Wind effect on the VRA is a critical factor in the design of a building. To address this issue, the National Research Council of Canada (NRC), in collaboration with members of the roofing industry and vegetated system manufacturers, initiated a standard development study. The main objective of this collaboration is to evaluate the wind uplift performance of VRA and to develop a national standard for possible inclusion into the building codes. This presentation will report the progress made on this project.

Speaker

Appupillai "Bas" Baskaran, PhD, PEng — National Research Council

BAS BASKARAN is a group leader at the NRC, where he is researching the wind effects on building envelopes through experiments and computer modeling, and is a research advisor to various task groups for the National Building Code of Canada. As an adjunct professor at the University of Ottawa, he supervises graduate students. He is a member of RICOWI, RCI, ASCE, SPRI, ICBEST, and CIB technical committees and a member of the Wind Load Committee of ASCE. He has authored over 200 research articles in the area of wind effects on buildings and has received more than 25 industry awards.

Nonpresenting Coauthors

Sudhakar Molleti, PhD — National Research Council

SUDHAKAR MOLLETI is a research officer in the Roofing Group of the Performance of Roofing Systems and Insulation (PRSI) of the NRC. He is currently researching the wind performance of vegetated roof assemblies, energy and durability performance of PV-integrated roofs, and application of vacuum insulation panels (VIPs) in roofing systems. Molleti is a member of the ASTM D08 and CRCA Technical Committees. He has a BS in civil engineering from the Gandhi Institute of Technology and Management, Andhra Pradesh, India, and master's and doctoral degrees from the University of Ottawa.

Fanella de Souza, PhD — National Research Council

FENELLA DE SOUZA is a research officer in the Bluff Body Aerodynamics Group of NRC Aerospace. Her work focuses on wind engineering, including building and ground vehicle aerodynamics. She received her BS degree in mechanical engineering from McGill University, Montreal, Canada; her master's in mechanical engineering from the University of Ottawa, Canada; and her PhD in aerodynamics from the Centre d'Études Aerodynamiques et Thermiques, Université de Poitiers, France.

Development of a Standard Test Method to Determine the Wind Resistance of Vegetated Roof Assemblies

BACKGROUND

A roof is an integral part of a building envelope. Roof slope less than 14° constitutes a low-sloped roof, which is commonly found on institutional, commercial, and industrial (ICI) buildings. A roof system (RS) on a low-sloped roof integrates several components, such as waterproofing membrane, insulation, and barriers, to the structural support. The large footprint of ICI buildings makes the RS an excellent platform for both energy harvesting and energy mitigation techniques. One of the growing movements in energy reduction, reduced greenhouse gases (GHG), and improved aesthetic value for the building is the installation of vegetated systems (VS) on the RS. These consist of a variety of components, such as growing media, drainage layers, and plants. The combination of RS and VS assembled together is defined as a vegetated roof assembly (VRA.) (See *Figure 1*.)

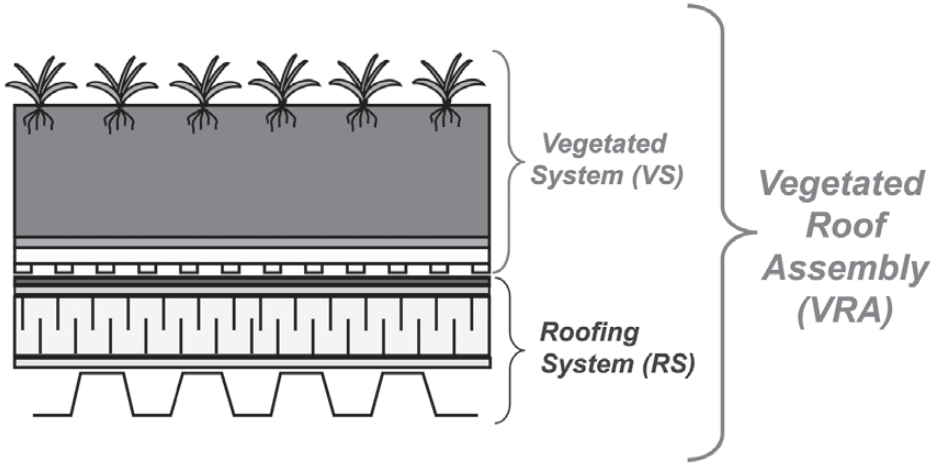

Figure 1 – Defining a VRA.

Within the category of low-sloped roofing, two main types of roofs are in use. One is the conventional system, where the waterproofing membrane is on the top, exposed to the environmental effects and with the thermal barrier and other roofing components below it; and the other is the protected membrane roof (PMR) system, with the membrane placed below the insulation. Both roof types are favorable for the installation of vegetated systems. This paper focuses on the VRA installed over conventional roofing systems.

Differences in the vegetated systems types exist, such as:

- Modular systems, where vegetation is pre-grown and components are engineered in movable, interlocking grid arrangements
- Pre-cultivated mats, with growing medium and plants rolled onto the roofing system with drainage mats and root barriers as required
- Built-up systems, where each component of the system (i.e., drainage layers, filter cloth, growing media, and plants) is installed separately

Each type of vegetated system has its own benefits[1]; however, what is important is how well they blend with the building design and roofing system in resisting the wind forces. The variability is greater in the case of the built-up systems compared to other systems; hence, it is excluded from the present study.

The prerequisite for the wind uplift design of VRA is that its resistance should be greater than its design load.[2] In Canada, the roof cladding design load, which is a function of various parameters such as roof structure, slope, wind speed, building height, building terrain, build-

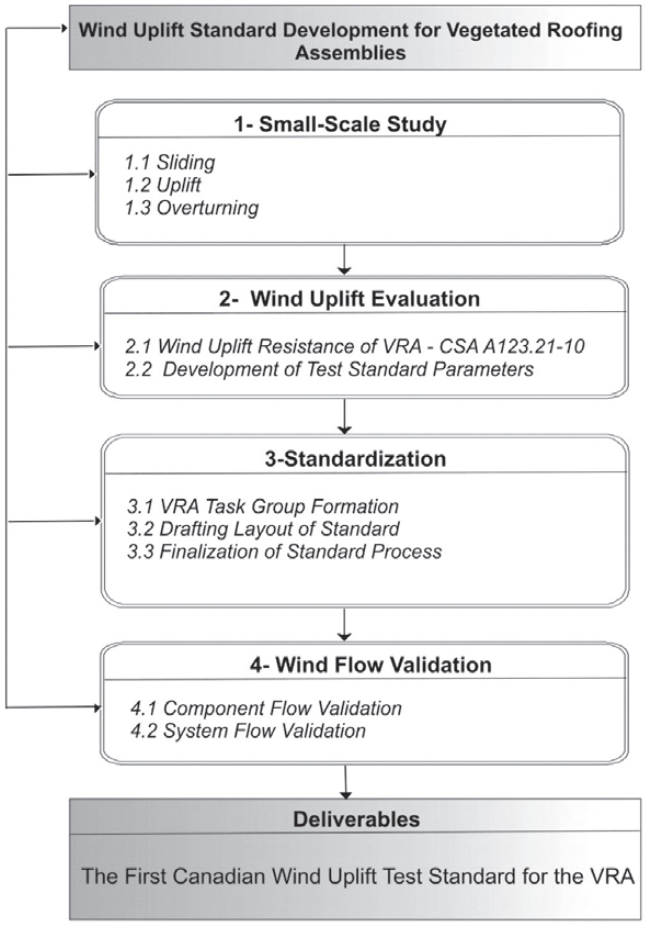

Figure 2 – VRA project outline.

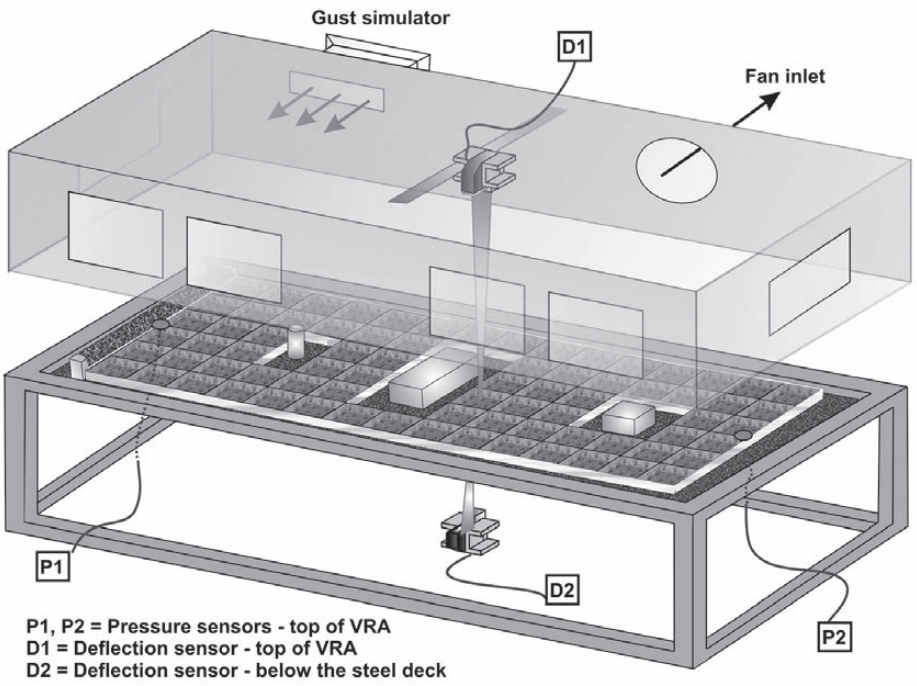

Figure 3 – Dynamic roofing facility (width = 16 ft. [4.9 m]; length = 32 ft. [9.8 m]).

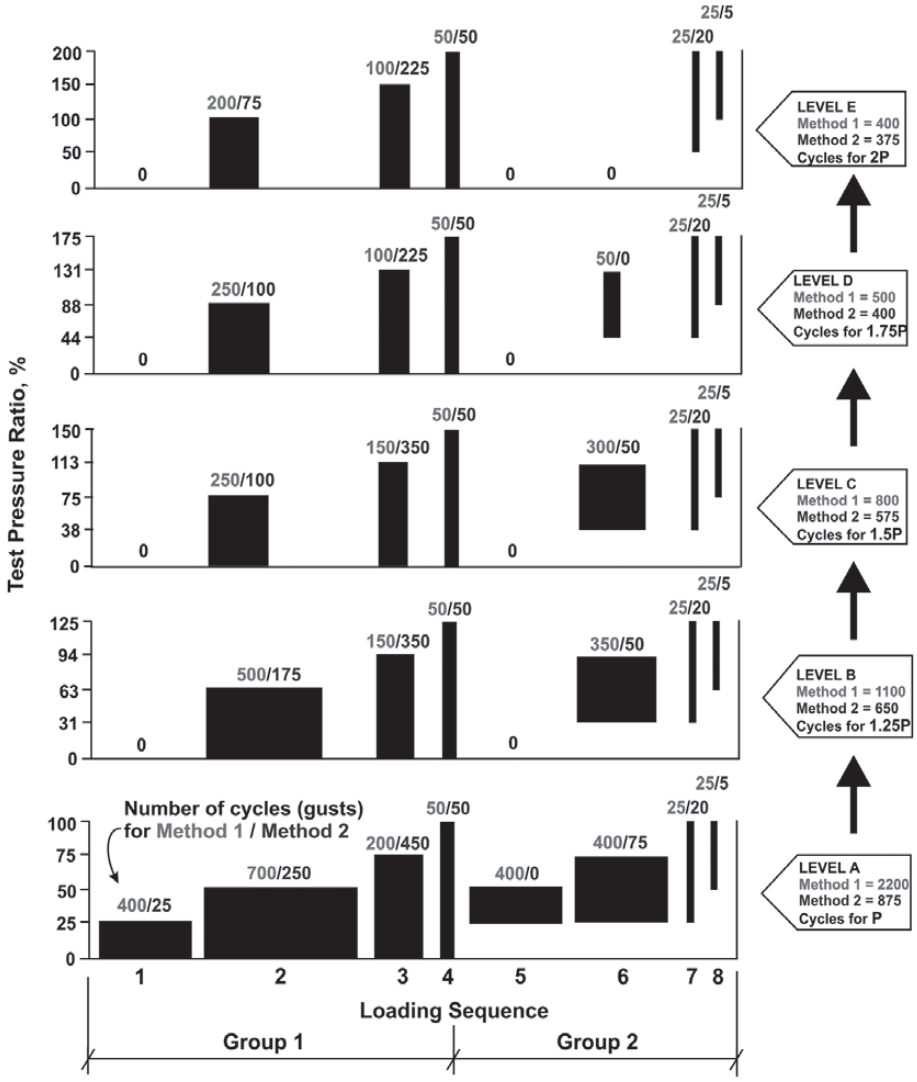

Figure 4 – CSA dynamic loading cycle.

ing type, and building openings—is determined from the National Building Code of Canada (NBC) 2010. To ease the process, NRC, in collaboration with the Special Interest Group for the Dynamic Evaluation of Roofing Systems (SIGDERS), developed an Internet-based tool for roof cladding wind design (WINDRCI; visit www.sigders.ca). From the resistance perspective, no technical standard exists to determine the wind uplift rating of the VRA. The existing literature refers to documents from NRCA,[3] ANSI/SPRI-RP14,[4] ANSI/GRHC/SPRI VR-1,[5] FEMA P-757,[6] FM 1-35,[7] and Prevatt et al. (2012)[8]. It should be noted, however, that these documents are only design guidelines and offer little to building officials to determine pass/fail criteria as a consensus-based standard will do. There is no tool available for both the roofing community and the vegetated system manufacturers to demonstrate the wind uplift compliance with the requirements of the building codes. This high-risk factor impedes the adoption of vegetated roofing technology and limits its use and growth.

To evaluate the coherent wind uplift performance of VRA, the NRC, in collaboration with members of the Canadian roofing industry and vegetated system manufacturers, has initiated a standard development study. The main objective of this collaboration is to develop a national wind uplift standard for VRA for possible inclusion into the building codes.

RESEARCH APPROACH

The project has four main tasks, and *Figure 2* highlights the subtasks involved:

Task 1: Small-scale study
Task 2: Wind uplift evaluation
Task 3: Standardization process
Task 4: Wind flow validation

To address these tasks, data were collected based on two sets of experiments:

1. Wind uplift resistance
2. Wind flow resistance

In wind uplift resistance, the VRA is subjected to dynamic wind-induced suctions in a confined test chamber. It quantifies the uplift deformation of the above-deck components and the uplift resistance of the VRA.

In wind flow resistance, the emphasis is on the flow dynamics' impact on the VRA. In controlled wind flow conditions, the uplift

Figure 5 – A typical VRA installation at the DRF-xL.

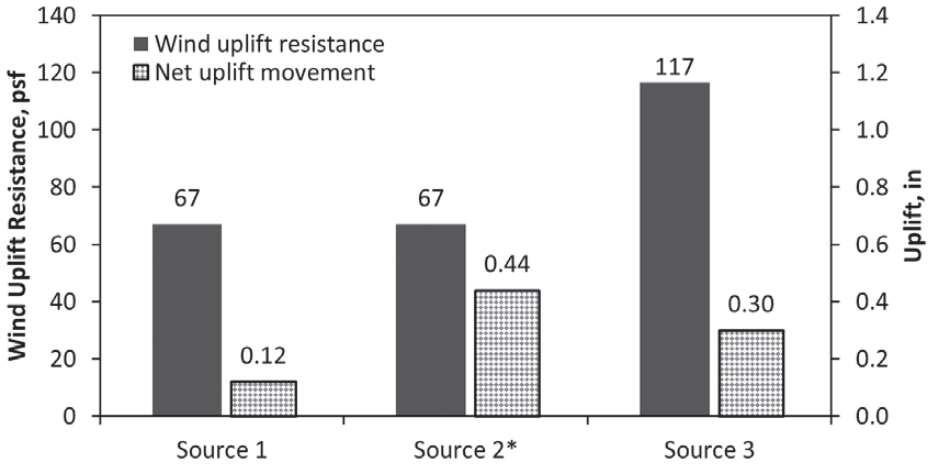

**Note: Source 2 did not pass Level A as the net uplift deformation is greater than 0.30 in*

Figure 6 – Wind uplift resistance of VRA.

and lateral sliding of the VS components are quantified. The pressure distribution across the VS and RS is measured, and the net uplift coefficient is determined.

The detailed experimental approaches are described below.

WIND UPLIFT RESISTANCE

Experimental Setup

All experiments were carried out at the NRC's Dynamic Roofing Facility (DRF-xL) (*Figure 3*). The details about the facility were documented in 2009 by Baskaran et al.[9] The testing was conducted in accordance with the CSA A123.21-14 dynamic test protocol[10,11] (*Figure 4*). Three VS from three different sources (1, 2, and 3) were evaluated with different combinations of RS to obtain a wind uplift rating of the respective VRA. The VS were plastic module trays. The RS comprised 22-Ga, 80-ksi steel deck, vapor barrier, insulation, cover board, and membrane. With these three sources, six different assemblies were tested. All the tested assemblies had three rooftop penetrations—a pipe and two curbs—and a parapet in their assembly layout (*Figure 5*). The instrumentation was comprised of pressure and deflection sensors to measure the response of the VRA (*Figure 3*). Assemblies were constructed by the participating members.

Experiment Observations and Results

Establishment of failure criteria is critical in the wind uplift resistance evaluation. In the VRA, the VS configuration allows for pressure equalization for the wind-induced dynamic pressures. In other words, the modular arrangement of the VS—i.e., the gap between modules and the roof membrane surface—allows for equalization of pressure. Depending on the ratio of pressure equalization and its relation to the resisting force (weight of VS module), uplift or overturning of the VS can occur. The dynamic testing protocol of CSA A123.21 simulates wind suction uniformly across the testing table. During the testing, it was observed that pressure equalization occurs above and below the VS, and therefore the overturning of the modules did not occur. Consequently, the wind uplift performance of the VRA was evaluated based on two criteria: 1) failure of the RS and 2) maximum allowable uplift deformation of above-deck components. The net uplift deformation (D1-D2) of the above-deck components, including VS, was measured by installing deflection sensors below (D2) and above the VRA (D1). The tests were carried out until the failure of the test specimen or when the D1-D2 exceeded 2L/240, where L is the deck structural span. For the present study, a 6-ft. (1.8-m) span was maintained; and thus, 2L/240 = 0.6 in. (15.2 mm).[12]

It should be noted that VRA has to sustain all the dynamic loading sequences of Level A of the CSA protocol to attain wind uplift rating, and that rating normalized by a factor safety of 1.5 is the wind uplift resistance of the VRA. The allowable uplift deformation of the above deck component is limited to L/240; with the present study, it is equal to 0.3 in. (7.6 mm). *Figure 6* summarizes the wind uplift resistance of the VRA.

For **Source 1**, two assemblies were tested. Assembly 1 failed at Level A, Sequence 4 at a suction pressure of 76 psf (3.6 kPa). The deflection data of D1 and D2 indicate that D1 measured higher deflection than D2, which implies that the RS had undergone some failure that led to this higher net deflection. This was confirmed by the visual failure that was observed during the testing. Assembly 1 failed due to fastener plate pull through the cover board. Comparing the initial deflections at 25 and 50 psf (1.2 and 2.4 kPa) indicated that D1 always measured higher deflections than D2. This indicated that kraft paper might not be minimizing air intrusion into the assembly and could have led to the failure of the cover board. As Assembly 1 did not sustain all the loading sequences of Level A, no rating was attained. In an attempt to make the substrate monolithic, Assembly 2 was constructed by mechanically fastening plywood sheets over the steel deck with 80 fasteners per board. Assembly 2 sustained Level A but failed at Level B. Sequence 3 obtained a wind uplift resistance of 67 psf. The pulling of the insulation plate through the insulation was the failure mode. The measured similar deflections of the D1 and D2 clearly indicate the monolithic behavior of this simulated roofing system.

For **Source 2**, three assemblies were tested: 3, 4, and 5. Assembly 3 was almost identical to Assembly 1 in the RS layout, with the exception of the vapor barrier/air retarder and the higher fastener density of the cover board. Self-adhered membrane was used as the vapor barrier/air retarder. The VS was different from Assembly 2, both in the module dimensions and weight and also in its installation layout. As mentioned above, due to pressure equalization, the difference in the VS installation does not have any impact on the wind uplift performance. Assembly 3 performed one notch higher than Assembly 1, failing at Level A, Sequence 4, at a suction of 100 psf (4.8 kPa). However, as it failed to meet

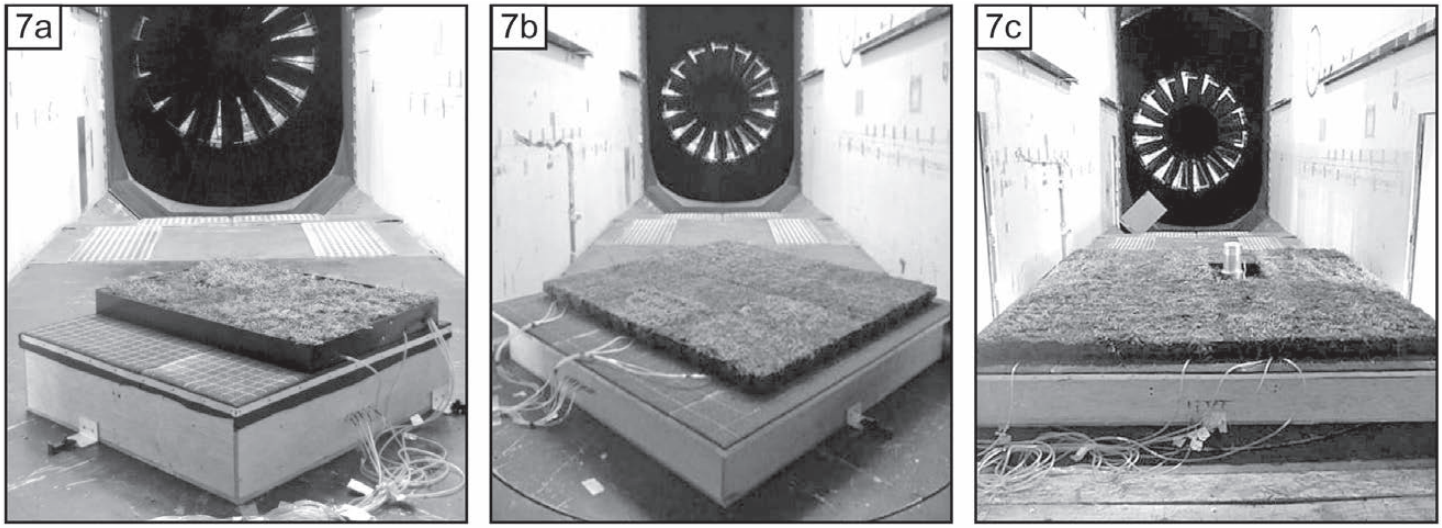

Figure 7 – Wind flow resistance test. 7a) 4 x 4 ft. with PE at 45-degree wind angle. 7b) 6 x 6 ft.; NPE at 45-degree angle. 7c) 8 x 8 ft.; NPE at 0-degree wind angle.

the Level A criteria, no rating was assigned to Assembly 3. This better performance could be attributed to the air-retarding effect of the self-adhered vapor barrier. However, at the higher suction, even the self-adhered vapor barrier could not minimize the air intrusion, making the cover board the weakest link and pulling the fastener plate through the board. Assembly 4 was the improved version of Assembly 3, replacing the asphaltic cover board with a prefabricated asphaltic cover board-base sheet composite. These prefabricated sheets were mechanically fastened with 16 fasteners per board, thus making the RS resilient. Assembly 4 was stopped at Level A, Sequence 3, when it was observed that the net uplift of the above deck components exceeded maximum allowable deflection of 2L/240 = 0.6 in. (15.2 mm). Assembly 4 was further enhanced by adding an additional row of fasteners on the cap sheet (Assembly 5). Regardless of enhancement, Assembly 5 did not pass Level A, as net uplift deformation exceeded L/240 = 0.3 in. (7.6 mm).

With the knowledge gained from the previous testing scenarios, **Source 3** tested only one assembly—Assembly 6, which had identical RS layout as Assembly 2. Simulating a monolithic substrate, more than 1,000 fasteners were used in fastening the plywood to the steel deck. A two-ply, modified-bituminous membrane was torched over the plywood, trying to mimic the behavior of a monolithic substrate. Assembly 6 was successful in resisting a wind uplift pressure of 117 psf (5.6 kPa).

It should be noted that the RS of Assemblies 2 to 6 are not representative of field construction of typical commercial roofing. Thus, the above-reported data should not be generalized for any type of monolithic substrate such as a concrete deck. For practical concrete deck applications, mimicking the structural strength of the concrete is important, as is its surface interaction (bonding strength and moisture ingress) with the membrane. In some cases, this could be the weakest link in the evaluation of VRA. Therefore, duplicating a field construction of the RS is very important in the wind uplift evaluation of VRA.

Although the investigations reported above provide some insight into the behavior of VRA, further studies are being conducted duplicating the field construction methodologies or component variations of the roofing system.

WIND FLOW RESISTANCE

Experimental Setup

The wind flow response of the VS was investigated at the wind tunnel facility located in Ottawa, Canada. The wind tunnel is a 9.8-ft. x 19.7-ft. (3-m x 6-m) open-circuit propulsion tunnel. It has a fan at its entry, and it permits test articles to discharge directly without recirculating or contacting the fan. With electric fan power, wind speeds up to 90 mph (40 m/s) can be attained. The wind tunnel is also equipped with a turntable, allowing testing at different wind angles.

The RS was a generic modified-bituminous roofing system, comprising a steel deck, vapor barrier, insulation, cover board, and membrane. For VS, only Source 2 was evaluated in this preliminary testing. Three parameters were investigated for the wind flow testing:

1. Effect of mock-up size
2. Effect of wind angle
3. Effect of perimeter edging

To determine appropriate specimen size for standard development, three different specimens were tested: 4 x 4 ft. (1.2 x 1.2 m), 6 x 6 ft. (1.8 x 1.8 m), and 8 x 8 ft. (2.4 x 2.4 m). Two wind directions: normal (0 degrees) and oblique (45 degrees) were investigated. The 8 x 8 ft. (2.4 x 2.4 m) mock-up could not be tested for oblique or 45-degree wind angle due to the size restriction of the tunnel. The impact of perimeter edging was quantified by testing the VRA with and without perimeter edging. The perimeter edging is a 26-Ga sheet metal bent at 90 degrees with 5- x 5-in. (127- x 127-mm) legs. With one type of VS and three roof mock-ups, a total of 10 tests were conducted. *Figure 7* shows the setup of the test mock-ups in the wind tunnel. The instrumentation contained pressure sensors installed on VS and RS, as shown in *Figure 8* for the 6- x 6-ft. (1.8- x 1.8-m) test specimen.

Test Protocol

With the specimen in position, the test is started with a wind speed of 30 mph (48 km/h). After attaining stabilization, the test speed is held for 60 seconds, and then it is ramped to the next speed level at increments of 10 mph (16 km/h). The test is continuous and moves from one speed level to another up to failure or up to 90 mph (145 km/h). An increment of 10 mph (16

km/h) was followed from 30 to 70 mph (48 to 112 km/h); and from 70 to 90 mph (113 to 145 km/h), the increment was reduced to 5 mph (8 km/h) to obtain better pressure distribution at higher wind speeds and also to capture the failure modes. The sustained wind speed is the test speed one level below the failure speed. It is normalized by a factor of safety of 1.5 to determine the wind flow resistance of the VS.

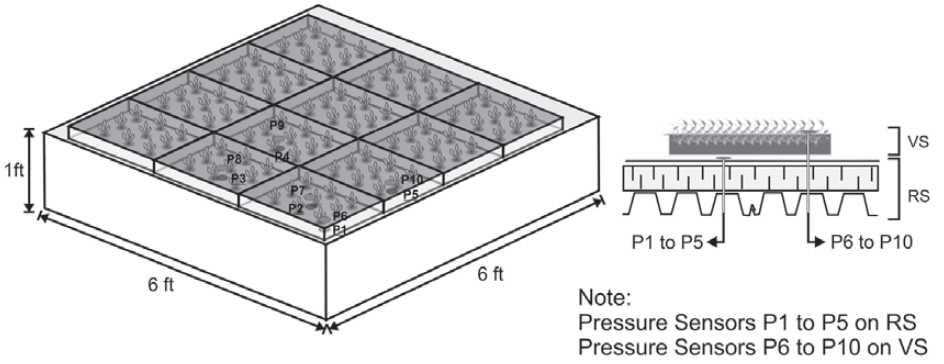

Figure 8 – Typical pressure sensors installation on VS and RS to quantify pressure equalization process.

Experiment Observations and Results

Figure 9 plots the wind flow resistance of the VS. The plotted data reflects the effects of the wind angle and perimeter edge on the wind flow resistance of VS. With no perimeter edge (NPE) and a 0-degree wind angle, irrespective of the mock-up size, the VRA sustained a wind speed of 56 to 58 mph (90 to 93 km/h). Turning the mock-up to 45 degrees, the VRA on the 4- x 4-ft. (1.2- x 1.2-m) mock-up failed earlier compared to 0-degree orientation, resisting a wind speed of 42 mph, while the VRA on 6- x 6-ft. (1.8 x 1.8-m) resisted the same wind speed as a 0-degree orientation before it failed. The failure mode in all the cases was the uplift and overturning of the modules.

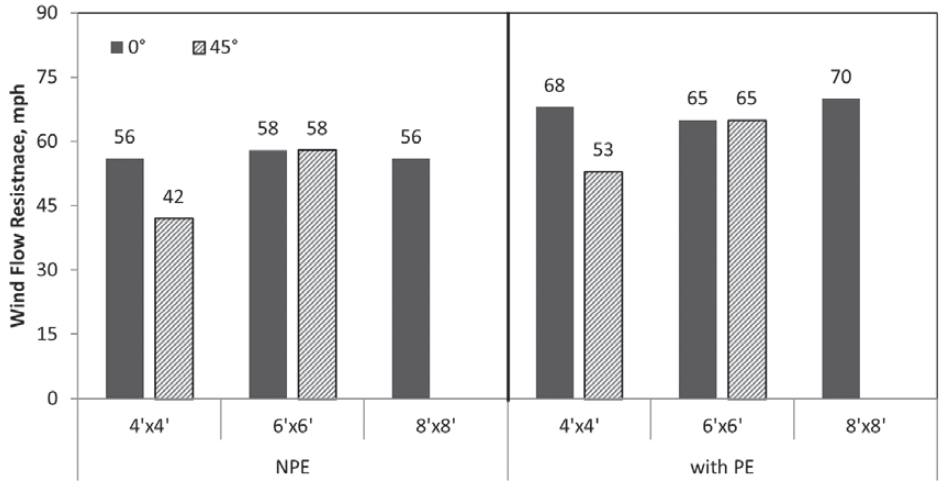

Figure 9 – Wind flow resistance of VRA.

The weight and design of the VS module is a critical parameter that contributed to the uplift of the modules. The VS design influences the pressure distribution across the VS, which in turn impacts its uplift force. The module uplift occurs when the aerodynamic uplift force on the module exceeds its self weight.[13,14,15] As the modules are not continuous and have gaps between them, in most cases, the air can readily enter around the edges, and the underside pressure can equalize with the surface pressure. The pressure equalization can have a direct impact in reducing the net uplift force on the module.

The pressure equalization or pressure ratio is the ratio of the RS pressure differential over the VRA pressure differential for a given location. However, in areas of very high spatial gradients of pressure, such as vortices near the roof corner, significant net uplift pressures can still occur on the modules, causing uplift. This phenomenon is well depicted in *Figure 10*, which clearly shows the relationship between pressure equalization and net uplift force for the scenario of NPE. When the approach wind to the VRA was normal, pressure equalization across M3 was almost 70% for all the wind speeds and M2 (which is behind M1) had almost 100% pressure equalization. This high pressure equalization mitigated the

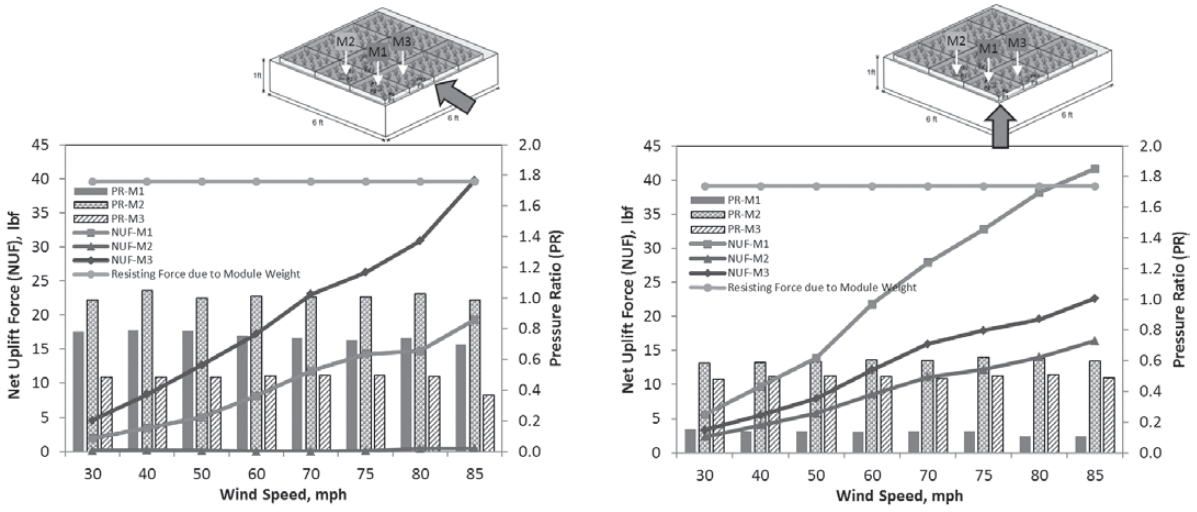

Figure 10 – Wind uplift force of 6 x 6 ft. NPE at 0 degrees (left) and at 45 degrees (right).

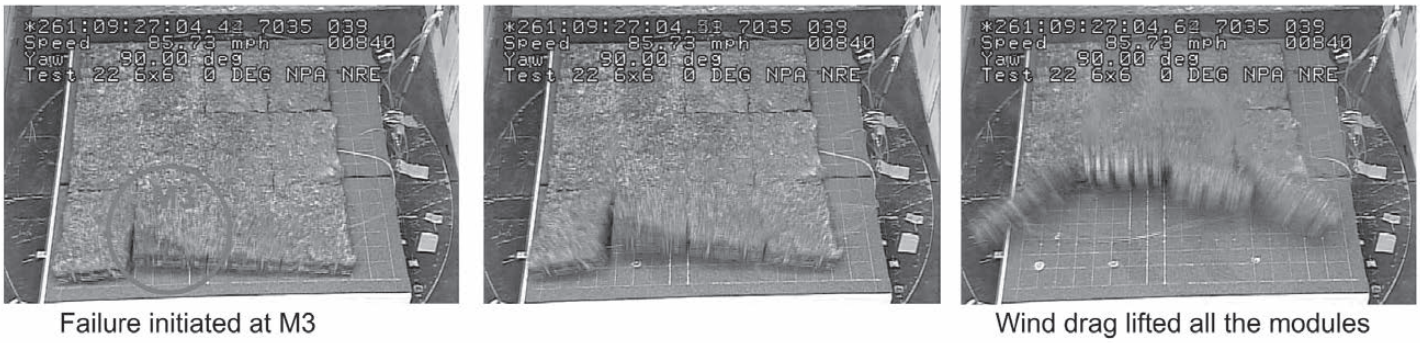

Figure 11 – Typical failure mode of 6 x 6 ft. NPE at 0-degree wind angle.

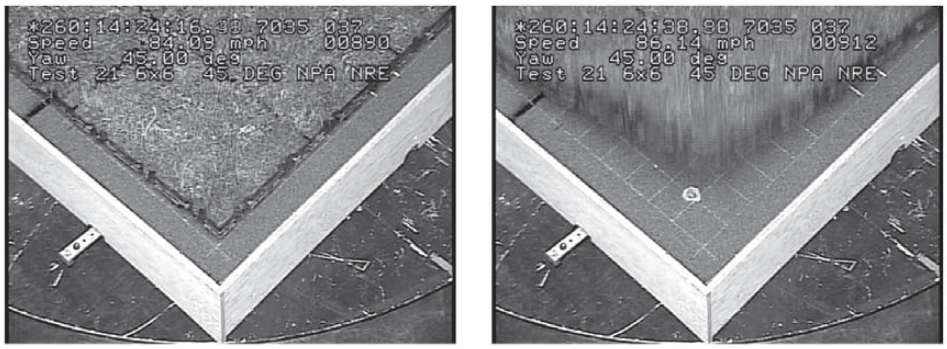

Figure 12 – Typical failure mode of 6 x 6 ft. NPE at 45-degree wind angle.

net uplift force on M1 and M2, which is less than the weight of the module. M3 (which is adjacent to M1) had only 50% pressure equalization. At an 85-mph (137-km/h) wind speed, there was a further drop in pressure equalization on M3. This increased the net uplift force. With the uplift force equal to the module weight, the module began to overturn and became airborne, as shown in *Figure 11*. Due to the interlocking mechanism between the modules, the wind drag lifted all adjacent modules, as shown in *Figure 11*. At a 45-degree wind angle, the aerodynamics were different. The corner vortices had a greater influence on M1, with pressure equalization as low as 10%. This resulted in higher net uplift force on M1, which led to the failure at 85 mph (137 km/h) when the net uplift force equaled the module weight (*Figure 12*).

When the perimeter edging (PE) was installed, there was considerable dampening change in the flow dynamics around the VS; thus the VS was then able to resist higher wind speeds up to 70 mph (113 km/h) without failure, except for the VS on the 4- x 4-ft. (1.2- x 1.2-m) mock-up, which failed at the 45-degree wind approach. *Figure 13* compares the performance of the VS with PE under the two different wind angles. First, irrespective of the wind approach angle, the presence of PE increased the pressure equalization compared to NPE. When the wind approach to the RS was normal, irrespective of the wind speed, M1, M2, and M3 had 60-100% pressure equalization. This resulted in lower uplift force on all three of the modules, keeping them in place without liftoff. Also note that the modules have an in-built interlocking mechanism, which allows the uplift load to be shared among the modules. This load-sharing is evident with the 45-degree wind approach. At 85 to 90 mph wind speed, the effect of corner vortices on M1 caused lower pressure equalization, with net uplift force exceeding the module weight. However, the interlocking of the modules allowed the uplift load on M1 to be shared between the adjacent modules, thus prevented M1 lift-off.

The 6- x 6-ft. (1.8- x 1.8-m) VRA mock-up showed a consistent performance in wind flow resistance. The aerodynamics of VRA with and without PE under different wind angles was well demonstrated through the relation between pressure equalization and net uplift force. For test standard development, the 6- x 6-ft. (1.8- x 1.8-m)

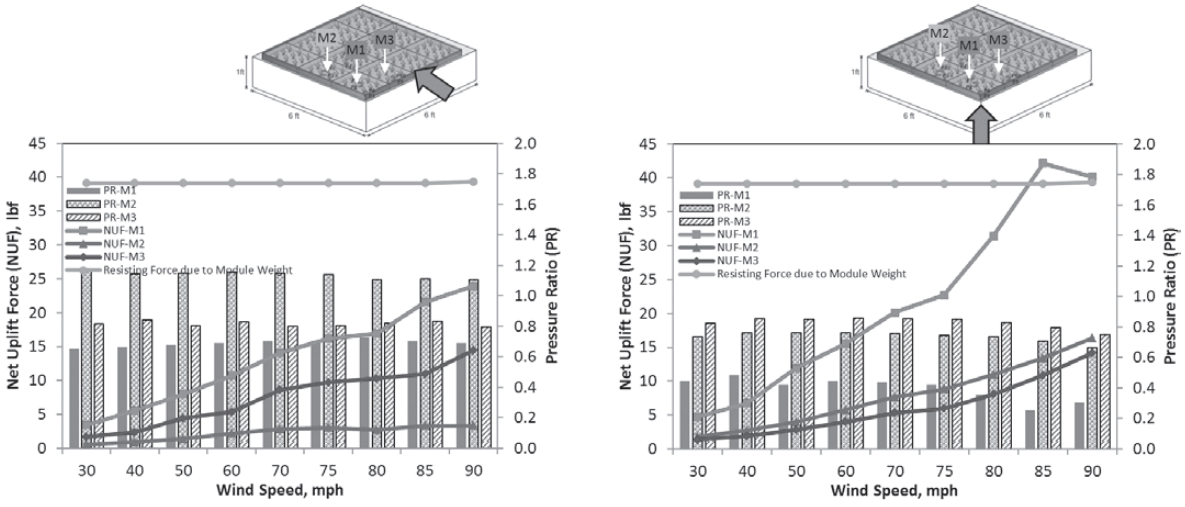

Figure 13 – Wind uplift force of 6 x 6 ft. PE at 0 degrees (left) and 45 degrees (right).

mock-up is identified as an optimum test specimen size with a 45-degree wind angle as the testing parameter representing the worst-case scenario. To simplify the standardization requirement, efforts are being made in translating this wind tunnel testing into laboratory testing with the tested benchmarked data.

CONCLUSION

A series of experiments have been conducted to investigate the VRA wind uplift resistance, as well as wind flow resistance. The wind uplift resistance testing identified the weakest links of the VRA and established failure criteria: failure of the RS and allowable uplift deformation of the above-deck component limited to L/240, where L is the deck structural span. The wind flow testing provided some key data towards understanding the wind aerodynamics acting on the VRA. The influence of corner vortices on the pressure distribution across VRA clearly showed that lift-off can occur when the aerodynamic uplift force exceeds the self weight of the VS. Installing a perimeter edge allows for pressure equalization that greatly reduces the net uplift force on the VS. These investigations provide information to assist in development of a national wind uplift standard for the VRA.

ACKNOWLEDGEMENT

The presented research is being carried out for a consortium called the Vegetated Roof Assembly (VRA). The VRA was formed by the Canadian Roofing Contractors' Association (CRCA) with partners Air-Ins, Armtec, Bioroof, the City of Toronto, the City of Ottawa, LiveRoof, Soprema Canada, Vitaroofs, and Xeroflor.

The contribution of the NRC technical team (P. Beaulieu, A. Duric, S.K.P. Ko, D. Van Reenen, and H. Yew) is greatly appreciated.

REFERENCES

1. A. Baskaran, D. Van Reenen, J. Overton, and K.K.Y. Liu, "Engineering Performance of Garden Roofs in North (Canadian) Climate – 5 Years of Field Data," *Proceedings of the RCI 24th International Convention & Trade Show*. Dallas, TX, March 12, 2009, pp. 1-6 (NRCC-50856).
2. A. Baskaran and T.L. Smith (2005), *A Guide for the Wind Design of Mechanically Attached Flexible Membrane Roofs*, www.nrc.gc.ca/virtualstore.
3. NRCA (2009), *The NRCA Vegetative Roof Systems Manual, Second Edition*, www.nrca.net.
4. ANSI/SPRI RP-14 (2010), *Wind Design Standard from Vegetative Roofing Systems*, www.spri.org.
5. ANSI/GRHC/SPRI VR-1 (2011), *Procedure for Investigating Resistance to Root Penetration on Vegetative Roof Systems*, www.spri.org.
6. FEMA P-757 (2009), "Mitigation Assessment Team Report: Hurricane Ike in Texas and Louisiana – Building Performance Observations, Recommendations and Technical Guidance."
7. FM 1-35 (2007), "Property Loss Prevention Data Sheets: Green Roof Systems," www.fmglobal.com.
8. D.O. Prevatt, G.A. Acomb, and F.J. Masters (2012), "Comprehensive Wind Uplift Study of Modular and Built-in-Place Green Roof Systems," Report No. UF01-12 submitted to Florida Building Commission.
9. A. Baskaran, S.K.P. Ko, and S. Molleti (2009), "A Novel Approach to Estimate the Wind Uplift Resistance of Roofing Systems," *Building and Environment*, 44, (4), pp. 723-735.
10. A. Baskaran, Y. Chen, and U. Vilaipornsawai (1999), "A New Dynamic Wind Load Cycle to Evaluate Flexible Membrane Roofs," *Journal of Testing and Evaluation*, 27 (4), pp. 249-265.
11. CSA A123.21-10 (2014), *Standard Test Method for the Dynamic Wind Uplift Resistance of Membrane Roofing System*, www.csashop.ca.
12. CSA A123.24-14 (2014), *Standard Test Method for the Dynamic Wind Resistance of Vegetated Roofing Assemblies* (www.csa.ca; in balloting process).
13. B. Bienkiewicz and Y. Sun (1992), "Wind Tunnel Study of Wind Loading on Loose-Laid Roofing Systems," *Journal of Wind Engineering and Industrial Aerodynamics*, Vol. 41-44, pp. 1817-1828.
14. K.K. Bofah, H.J. Gerhardt, and C. Kramer (January 1996), "Calculations of Pressure Equilibrium Underneath Loose-Laid Flow Permeable Roof Insulation Boards," *Journal of Wind Engineering and Industrial Aerodynamics*, Vol. 59, Issue 1, pp. 23-37.
15. R.J. Kind, M.G. Savage, and R.L. Wardlaw (September 1987), "Pressure Distribution Data Measured During the September 1986 Wind Tunnel Tests on Loose-Laid Roofing Systems."